SECOND EUROPEAN CONFERENCE ON EARTHQUAKE ENGINEERING
AND SEISMOLOGY, ISTANBUL AUG. 25-29, 2014

SIMULATION OF RC WALLS SEISMIC BEHAVIOUR WITH SHELL ELEMENTS AND PARC_CL MODELLING

Beatrice BELLETTI[1] , Cecilia DAMONI[2] , Matteo SCOLARI [3] and Alessandro STOCCHI [4]

ABSTRACT

The structural response of reinforced concrete (RC) wall system is usually characterized by low displacement values at the damage and ultimate limit states; such systems are then quite common in industrial and power plant buildings.

The paper presents for some case studies a brief review of experimental tests available in literature and non linear finite elements (NLFE) methods for pushover analysis. In particular, in the paper a multi-layered shell model based on the fixed crack approach PARC_CL (Physical Approach for Reinforced Concrete under Cyclic Loading condition) is presented. Advantages and critical aspects related to shell modelling of wall systems are highlighted by multi-level assessment; in particular by comparing NLFEA results, obtained with the proposed shell element modelling, with experimental observations, NLFEA results obtained with beam element modelling and analytical formulations prescribed by Eurocode 8 (EC8). In the paper it is demonstrated that multi-layered shell modelling can be a numerical tool for the analysis of different structural wall typologies, like ductile wall systems (coupled or uncoupled), dual systems (frame or wall equivalent) and squat or large wall systems.

1 INTRODUCTION

Structural wall systems are commonly used both in day to day and industrial power plant design. In civil buildings structural slender walls systems are common because they provide strength and stiffness towards seismic actions allowing a good displacement control (Riva et al., 2003). Squat walls and low rise walls are widespread in buildings realised with precast concrete blocks and in power plant facilities as main horizontal resisting structures (Whyte and Stojadinovic, 2013).

From 1976 to 1984 Oesterle et al. (1976) tested many slender walls subjected both to monotonic and cycling loading in order to evaluate their inelastic behaviour. In these tests flanged, barbell and rectangular sections were analysed. Many other studies have been carried out to test the behaviour of slender walls towards lateral seismic forces. Some studies concerning slender walls are for example CAMUS (1995-1998), UCSD: NEES benchmark (2005-2006), LNEC Ecoleader (2003-2005).

Many experimental studies have been carried out in order to assess the behaviour of RC shear and squat walls. Such experimental campaign have been reviewed and summarized throughout the years by some authors and in PhD theses (Wood 1990, Martinelli 2007, Grifenhagen 2006 and Gulec 2009). Experimental tests, as reviewed by Wood and Martinelli, have been run mainly considering monotonic, repeated and alternating loading. Regarding low rise walls or squat and large walls many experimental tests have been run from the ‘70s (Barda et al. 1977, Maier and Thurlimann, 1985, Lefas

[1] Assistant Professor, University of Parma DICATeA, Parma, Italy, beatrice.belletti@unipr.it
[2] PhD, University of Parma DICATeA, Parma, Italy, cecilia.damoni@gmail.com
[3] PhD Student, University of Parma DICATeA, Parma, Italy, scolari.matteo87@gmail.com
[4] PhD Student, University of Parma DICATeA, Parma, Italy, ing.stocchi@gmail.com

and Kotsovos, 1990). Recently, tests have been run by Pilakoutas and Elnashai (1993) on specimen with aspect ratio equal to 2 subjected to severe cyclic loading, by Gupta and Rangan (1998) on high strength concrete HSC shear wall subjected to monotonic lateral loads, by Kabeyasawa and Hiraishi (1998) on flanged HSC walls with aspect ratio approximately equal to 2, by Palermo and Vecchio (2002) on squat flanged shear walls under cyclic displacement, by Farvashany (2004) on HSC shear wall with aspect ratio 1.25 subjected to monotonic loading. It can be noted that only few pseudo-dynamic tests are available in literature. Naze and Sidaner (2001) analysed, within the SAFE project, the dynamic behaviour of very squat walls (with aspect ratio 0.4). Also Mazars et al. (2002) conducted significant studies, starting from the results of the SAFE project tests.

In the design practice the structural analysis of RC walls systems, especially when software aided, is carried out modelling RC wall systems with equivalent beams. Indeed, the traditional structural analysis of frame systems is well known in engineering practice and it is also used to carry out safety verifications of ductile wall systems (coupled or uncoupled) and dual systems (frame or wall equivalent), by transforming the walls behaviour to equivalent columns behaviour. Sometimes, due to the geometrical features of RC walls, the Bernoulli hypotheses are not suitable for the description of the real walls behaviour, even in case of ductile walls, because walls are principally constituted of discontinuity regions. Furthermore the shear resistance (especially near supports and floors), the flexural bending resistance and the curvature ductility determination (especially for composite wall cross sections like "U", "L" and "C" shapes) requires a-priori assumptions to be performed with beam modelling. Standard codes recommend the use of variable inclination truss models or the use of a strut and tie model only for the evaluation of the shear resistance of shear walls.

The structural analysis of RC walls with plate or shell elements modelling is currently adopted to carry out linear and non-linear dynamic or equivalent static analyses of wall systems or dual systems (Palermo and Vecchio, 2007).

The paper focuses on the prediction of the non-linear behaviour of RC walls systems with multi-layered shell elements and total strain smeared crack models. Numerical results obtained with DIANA Code and ABAQUS Code will be presented; in particular a multi-layered shell element model, developed at the University of Parma using the finite element code ABAQUS will be illustrated. The latter procedure adopts PARC_CL model, implemented in the user subroutine UMAT.for of ABAQUS Code, to evaluate the non-linear stiffness matrix at each integration point.

In the paper a multi-story building will be adopted as case study to demonstrate that for ductile walls the structural response at collapse can be predicted with similar level of accuracy by adopting shell element models or beam element models (by adopting distributed plasticity models or lumped plasticity models). However, the modelling with shell elements and smeared crack models can be more powerful, if compared to other approaches, for the structural assessment of shear walls and wall buildings characterized by both brittle shear or torsional failure and ductile bending failure. Thus in the paper the case studies of the Concrack 4 shear wall (Damoni et al. 2013, Belletti et al., 2013[a]) and of a ductile wall tested at the University of Brescia will be presented to illustrate that the shell elements modelling with smeared crack models can properly predict the indicators of damage, in particular local engineering demand parameters like concrete and rebar strains and crack opening values, and global engineering demand parameters like displacement values, which are fundamental for the application of performance-based earthquake engineering,

In the paper analytical provisions and definitions provided by EC8 for the resistance evaluation of RC walls are reported and finally, for each case study, analytical resistance values are compared to NLFEA results.

2 THE PROPOSED MULTI-LAYERED SHELL ELEMENT AND PARC_CL MODELLING

It is well known that NLFE analyses allow for more realist modelling of material and structural behaviour and, in this manner, can account for additional bearing capacity of the structure. Nevertheless, the results obtained from NLFE analyses strongly depend on the assumptions made in the modelling steps (Damoni et al., 2013, Belletti et al., 2013[a]). The presented procedure adopts a multi-layered shell modelling where each layer behaves as an element subjected to plain state of

stresses. A total strain fixed crack model called PARC_CL (Belletti et al. 2013[b]), implemented at the University of Parma in the user subroutine UMAT.for for ABAQUS code, has been used to evaluate the mechanical non-linearity of RC layers. PARC_CL model is an evolution of the PARC model (Belletti et al. 2001). PARC_CL model describes the behaviour up to failure of reinforced concrete structures subjected to loading-unloading-reloading conditions. The adopted crack model is tailored to analyse structures failing in shear. Strain penetration effects are not incorporated in the actual version of the model.

2.1 PARC_CL crack model

The PARC_CL model is based on a total strain fixed crack approach, in which at each integration point two reference systems are defined: the local x,y coordinate system and the 1,2 coordinate system along the principal stress conditions. The angle between the 1-direction and the x-direction is denoted as ψ, whereas $\alpha_i = \theta_i - \psi$ is the angle between the direction of the i-th order of the bar and the x-direction. When the maximum tensile principal stress reaches the concrete tensile strength f_{ct}, cracking starts to develop, and the 1,2 coordinate system is fixed (Fig. 1).

The concrete behaviour is assumed to be orthotropic, both before and after cracking; softening in tension and compression, a multiaxial state of stress and the effect of aggregate interlock are taken into account. The reinforcement is modelled through a smeared approach; dowel action and tension stiffening phenomena are considered.

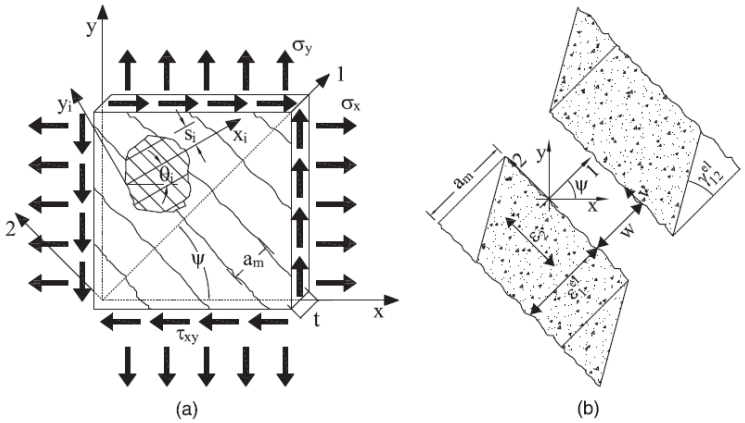

Figure 1. a) Reinforced concrete element subjected to plane stress state; b) kinematic quantities.

The total strains at each integration point are calculated, in the 1,2 coordinate system, as the sum of the elastic (superscript *el*) and the inelastic (superscript *cr*) strains.

$$\varepsilon_1 = \varepsilon_1^{el} + \varepsilon_1^{cr} = \varepsilon_1^{el} + w/a_m \tag{1}$$

$$\varepsilon_2 = \varepsilon_2^{cr} \tag{2}$$

$$\gamma_{12} = \gamma_{12}^{el} + \gamma_{12}^{cr} = \gamma_{12}^{el} + v/a_m \tag{3}$$

where w=crack opening, v=crack sliding and a_m=crack spacing calculated through an a priori method, Leonhardt and Schelling (1974), based on the transmission length of bond between concrete and steel. The strains in the x,y coordinate system, $\{\varepsilon^{(x,y)}\}$, are obtained through the transformation matrix $[T_\varepsilon]$ which is a function of the fixed angle ψ.

The overall stiffness matrix in the x,y coordinate system, $[D^{(x,y)}]$, is obtained by assuming that concrete and reinforcement behave like two springs placed in parallel, Eq.(4).

$$\begin{aligned}\left[D^{(x,y)}\right] &= \left[T_\varepsilon\right]^T \left[D_c^{(1,2)}\right]\left[T_\varepsilon\right] + \left[T_{\theta i}\right]^T \left[D_s^{(x_i,y_i)}\right]\left[T_{\theta i}\right] \\ &= \left[T_\varepsilon\right]^T \begin{bmatrix} \overline{E}_{c1} & 0 & 0 \\ 0 & \overline{E}_{c2} & 0 \\ 0 & 0 & \beta G \end{bmatrix}\left[T_\varepsilon\right] + \left[T_{\theta i}\right]^T \begin{bmatrix} \rho_i \overline{E}_{si} g_i & 0 \\ 0 & \rho_i d_i \end{bmatrix}\left[T_{\theta i}\right]\end{aligned} \tag{4}$$

In Eq. (4) the concrete stiffness matrix $[D_c^{(1,2)}]$ is defined in the 1,2 coordinate system, as a function of the concrete contribution in tension and in compression ($\bar{E}_{c1}$ and $\bar{E}_{c2}$) and of the aggregate interlock effect (βG). The steel stiffness matrix $[D_s^{(xi,yi)}]$ is defined, in the x_i, y_i coordinate system, as a function of a reinforcement contribution ($\bar{E}_{si}$) and tension stiffening (g_i). The transformation matrixes $[T_\varepsilon]$ and $[T_{\theta i}]$ are used to rotate the concrete matrix from the 1,2 to the x,y coordinate system and the steel matrix from the x_i, y_i to the x,y coordinate system, respectively.

The stresses $\{\sigma^{(x,y)}\}$ in the x,y coordinate system are defined by multiplying the stiffness matrix $[D^{(x,y)}]$ and the strain vector $\{\varepsilon^{(x,y)}\}$. The constitutive model PARC_CL allows secondary cracking perpendicular to primary cracking by imposing E_{c2} equal to zero.

The concrete and steel behaviour as well as their interaction effects are modelled with constitutive relationships for loading-unloading- reloading conditions. In this paper, only the concrete constitutive law and the aggregate interlock relation are described. For more details regarding the other constitutive relations used in the PARC_CL model refer to (Belletti and Esposito, 2010).

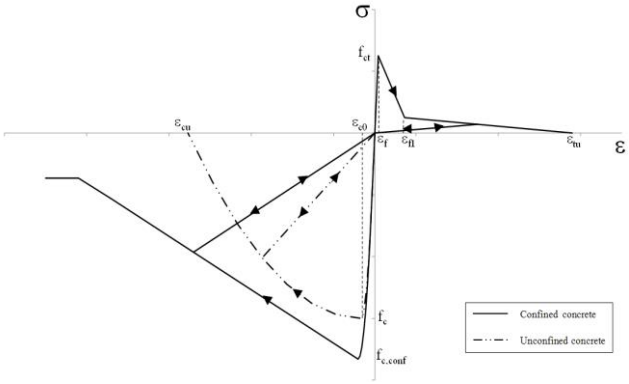

Figure 2. Constitutive model for concrete (not to scale).

The stress-strain relationship for un-confined concrete (Fig. 2) is described by Eq.(5).

$$\sigma = \begin{cases} E_c\varepsilon & 0 \le \varepsilon < \varepsilon_f \\ f_{ct}\left[1+0.85\left(\varepsilon-\varepsilon_f\right)/\left(\varepsilon_f-\varepsilon_{f1}\right)\right] & \varepsilon_f \le \varepsilon < \varepsilon_{f1} \\ 0.15 f_{ct}\left[1+\left(\varepsilon-\varepsilon_{f1}\right)/\left(\varepsilon_{f1}-\varepsilon_{tu}\right)\right] & \varepsilon_{f1} \le \varepsilon < \varepsilon_{tu} \end{cases} \quad \sigma = \begin{cases} \dfrac{E_c/E_{cs}-\varepsilon/\varepsilon_{c0}}{1+\left(E_c/E_{cs}-2\right)\varepsilon/\varepsilon_{c0}} E_{cs}\varepsilon & \varepsilon_{c0} \le \varepsilon < 0 \\ f_c\left[1-\left(\varepsilon-\varepsilon_{c0}\right)^2/\left(\varepsilon_{cu}-\varepsilon_{c0}\right)^2\right] & \varepsilon_{cu} \le \varepsilon < \varepsilon_{c0} \end{cases} \tag{5}$$

where E_c and E_{cs} are the initial modulus of elasticity and the secant stiffness corresponding to the peak strain ε_{c0}, respectively. The stress-strain relationship for concrete in tension is defined as a function of its tensile strength f_{ct}, the concrete strain at cracking ε_f, the strain ε_{t1} and ε_{tu} (corresponding to residual stress equal to $0.15f_{ct}$ and zero, respectively) and the fracture energy G_f in tension.

The compressive branch before reaching the peak is defined in agreement with Sargin relation and after the peak with Feenstra relation as a function of the concrete compressive strength f_c and concrete fracture energy in compression G_{fc}, assumed equal to 250 G_f, (Hendriks et al., 2012).

The Kent and Park (1971) relationship has been used for confined concrete.

Multi-axial state of stress is considered by reducing the compressive strength and the corresponding peak strain due to lateral cracking, as given in Eq. (6), (Vecchio and Collins, 1993):

$$\zeta = 1/\left(0.85-0.27\varepsilon_t/\varepsilon_{c0}\right) \tag{6}$$

being ε_t the tensile strain.

An elastic-plastic with hardening relation has been used for steel. The aggregate interlock effect (Fig.3) is evaluated on the basis of the crack width, w, and the crack sliding, v, following the relationship proposed by (Gambarova, 1983). For further details refer to (Belletti et al., 2013[a]).

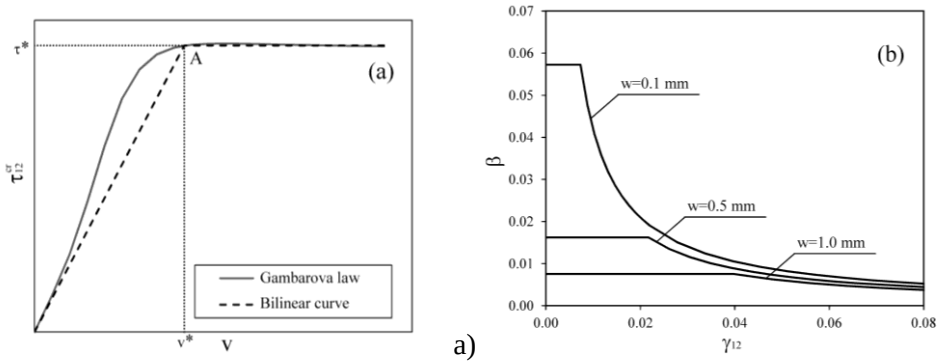

a) b)

Figure 3. Aggregate interlock model: a) shear stress-slip relationship, b) shear retention factor for different crack width values.

3 CASE STUDIES

3.1 Slender walls designed according to capacity design approach

The first case study presented in the paper concerns the analysis of a regular multi-story building, Fig.4. Three different models were adopted to perform pushover analyses. The first and simplest model was a lumped plasticity model implemented by the authors in Excel VBa at the University of Parma, denoted "LPA", the second one was a fibre-element model (implemented in Seismostruct software) and the third one was the multi-layered shell element model described in the previous session (Belletti et al., 2013[c]).

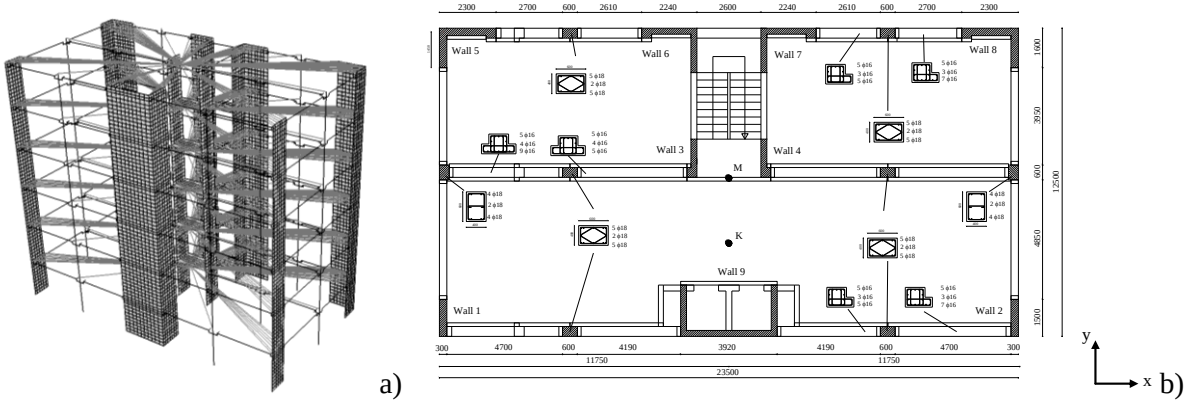

a) b)

Figure 4. a) Global model of a building with U-shaped, L-shaped and rectangular walls and b) building ground floor section.

3.1.1 Lumped plasticity model

For the lumped plasticity model the position of the resultant of lateral forces has been evaluated as given in Eq. (7):

$$H_e = \frac{\sum_{i=1,n} F_i \cdot z_i}{\sum_{i=1,n} F_i} \tag{7}$$

The moment – curvature relation is evaluated by referring to the cross section and the reinforcement at the base of the walls subjected to the axial force that derive from vertical loads. For each wall the moment versus curvature relation has been evaluated with the software Biaxial 1.3 by assuming an elastic-plastic behavior for longitudinal rebars and a parabolic stress-strain relation for concrete in compression. The resulting moment versus curvature relation is transformed into a base shear versus top displacement bi-linear relation, Fig. 5. The ultimate displacement $\Delta = \Delta_y + \Delta_p$ is

calculated on the basis of a yielding displacement Δ_y and a plastic displacement Δ_p respectively given by Eq.(8) and Eq. (9):

$$\Delta_y = \frac{\chi_y}{3} H_e^2 \tag{8}$$

$$\Delta_p = \left(\chi_u - \chi_y\right) \cdot L_{pl} \cdot \left(H_e - 0.5 \cdot L_{pl}\right) \tag{9}$$

where χ_y is the yield curvature and H_e the equivalent height of the wall.
The plastic hinge length is evaluated with Eq. (10):

$$L_{pl} = k \cdot H_e + 0.1 \cdot l_w + L_{sp} \tag{10}$$

being $k = 0.2 \cdot \left(f_u / f_y - 1\right) < 0.8$; $L_{sp} = 0.022 \cdot f_y \cdot d_{bl}$; d_{bl} the equivalent longitudinal rebar's diameter.

Finally the force – displacement relation can be drawn in Fig. 5 by assuming that $V_y = M_y / H_e$ and $V_u = M_u / H_e$. The capacity of the entire building can be obtained by applying the same procedure for all the walls, adding the contribution of single walls, in terms of shear base versus displacement, for each direction of the building, Fig. 6. In case of walls characterized by composite sections, the base shear versus displacement relations have been obtained for each principal axis of the transversal cross section and later combined through linear interaction diagrams in order to take into account for biaxial action effects.

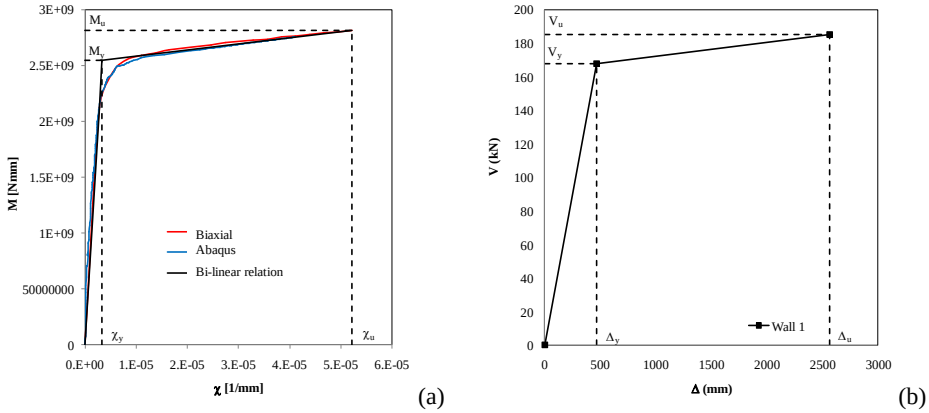

(a) (b)

Figure 5. (a) Moment versus curvature and (b) base shear versus displacement relations.

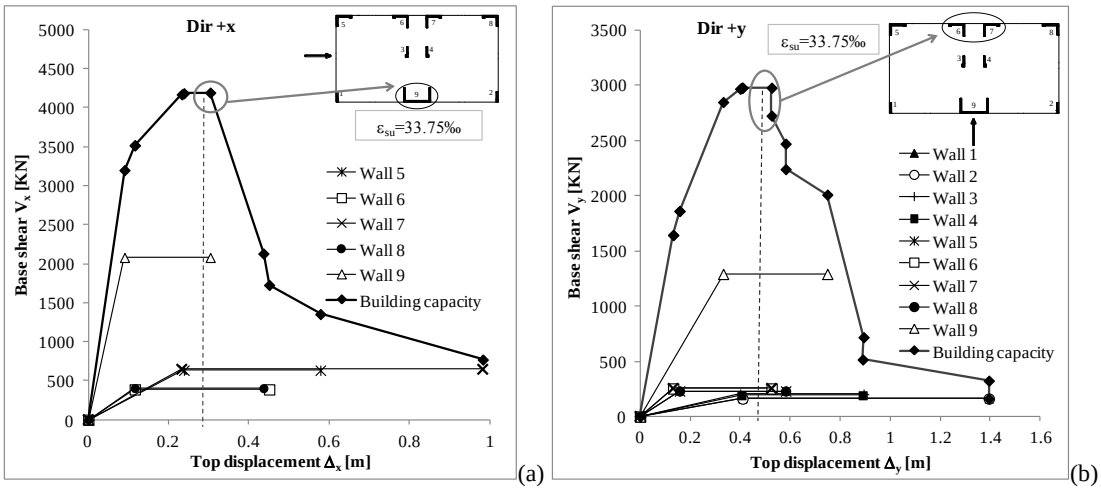

(a) (b)

Figure 6. Capacity curves of the building obtained with LPA considering only the rigid translation for seismic forces acting along (a) +x direction, (b) +y direction.

3.1.2 Distributed plasticity model

For the analyses carried out with Seismostruct software a uniaxial steel model based on stress-strain relationship proposed by (Menegotto and Pinto, 1973), coupled with the isotropic hardening rules proposed by (Filippou et al., 1983) is used for longitudinal rebars. An uniaxial nonlinear constant confinement model (Mander et al., 1988) is used for concrete. Two integration Gauss points per element are used for the numerical integration of the cubic formulation; each wall is subdivided in four elements per interstorey; the number of section fibres used in section equilibrium computations has been defined equal to 400. Lumped mass elements have been applied at each storey level and connected to wall. Masses and self-weight are automatically transformed to gravity loads for pushover analyses. The diaphragm behavior is modeled by imposing (with "EqualDOF" option) the same translations along *x* and *y* axes and rotation along *z* axis of the mass centroid to all nodes placed at the storey level. The response control option has been chosen as loading/solution scheme by controlling the response of the node at the mass centroid of the top of the building.

3.1.3 Discussion of the results obtained with the three procedures

In Fig.7 the capacity of the building, in terms of base shear vs total displacement curves, obtained with the three procedures previously described, is reported.

Fig.7(a) shows that when the seismic force acts along +x direction the first wall that collapses is wall 9 due to the reaching of the ultimate strain in reinforcing bars (ε_{su}=33.75 ‰), while when the seismic force acts along +y direction, Fig.7(b), the first walls that collapse are walls 6 and 7 due to the reaching of the ultimate strain in the reinforcing bars (ε_{su}= 33.75 ‰). The limit of 33.75 ‰ for the ultimate strain value in reinforcing bars has been chosen in order to take into account for buckling phenomena that could occur during cyclic loading. The contour plots illustrated in Fig.8 are in agreement with the failure mode obtained with the lumped plasticity model and with the distributed plasticity model.

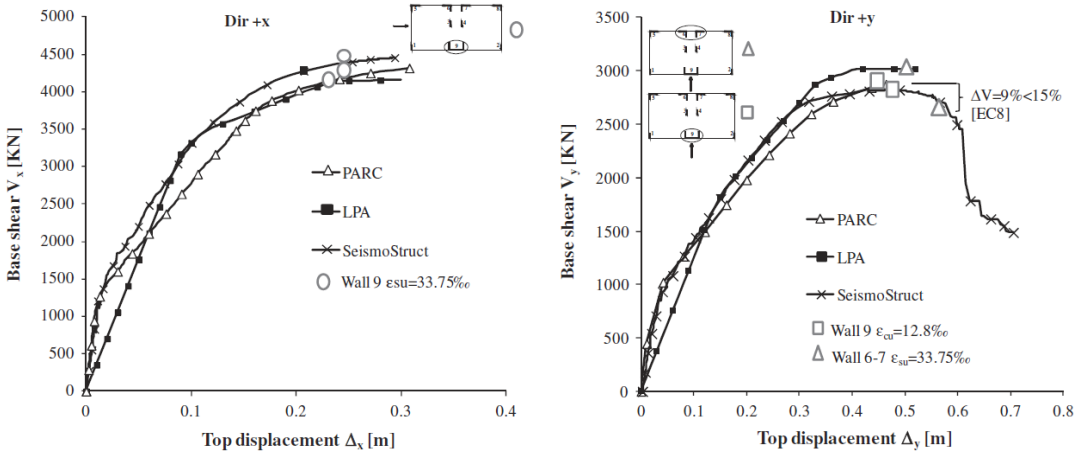

Figure 7. Shear-displacement diagrams for C-shaped and L-shaped walls according to different modelling techniques.

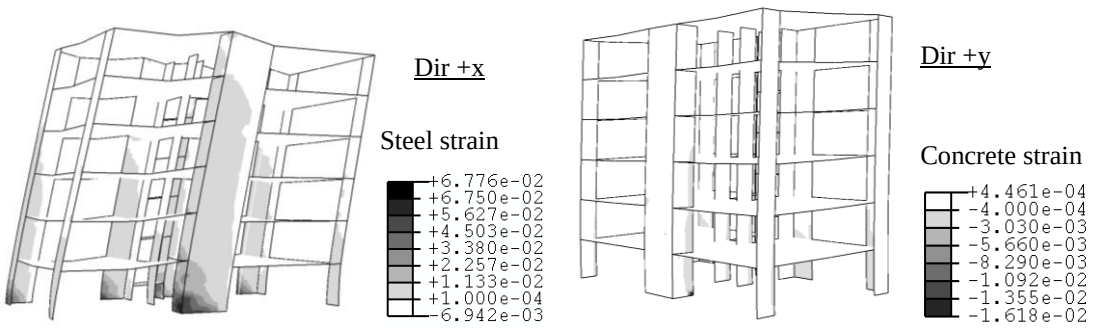

Figure 8. Steel and concrete strain at collapse detected in PARC model.

It can be noted that the shell modelling leads to a lower cracked stiffness than the stiffness obtained with distributed plasticity approach. This is due to the fact that the shell modelling is able to evaluate the effects of multiple state of stresses in concrete and shear interaction, which are neglected if an equivalent beam modelling of the wall is adopted.

In general, the results of the analyses carried out with the three models, even if they are based on different assumptions, demonstrate that the structural response at collapse can be predicted with similar level of accuracy in case of ductile wall systems of regular building designed according to capacity design approach. It is important to remember that only when the modelling of RC walls with equivalent beams can be properly adopted (that is only in case of slender walls with beams that can be considered simply supported to walls), the structural behaviour can be predicted with the same level of accuracy by the three previously described models. In that case the lumped plasticity models configures as a relatively simple model, applicable even for hand calculations in the daily design procedure. On the other hand, it should be remarked that in case of composite sections the shear capacity depends on the interaction between axial forces, bending moments and shear forces acting on flanges and webs, that can be properly evaluated with shell modelling (Ile and Reynouard, 2005). The interaction effects become more and more important in case of irregular buildings and in case of failure modes governed by shear.

3.2 Slender walls tested at the University of Brescia

A full scale wall, tested at the University of Brescia, Riva et al.(2003), Fig.9, has been modelled with the proposed multi-layered shell element approach (Belletti and Riva, 2008).

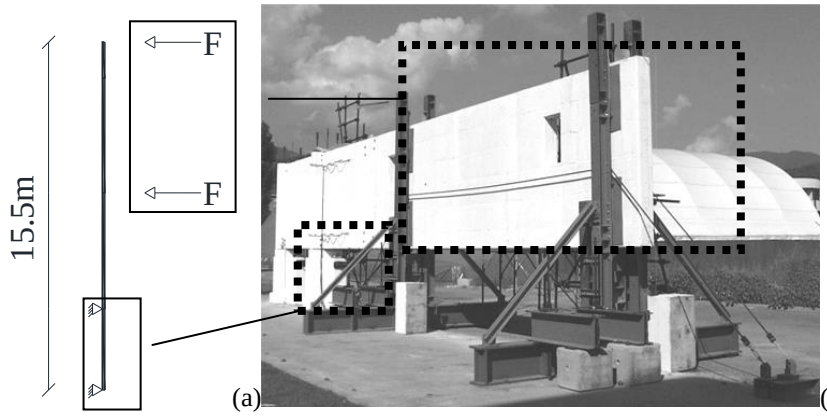

Table 1. Materials and geometrical parameters.

Parameter	Value
R_{cm}	40.7 MPa
h_w	11.5 m
l_w	2.8 m
t_w	0.4 m

Figure 9. (a) Static scheme of the load system, (b) a picture of the experimental test.

The web of the specimen was reinforced with Φ8/200 net corresponding to a reinforcement ratio ρ_h = 0.17% lower than the minimum prescribed by EC8, equal to $\rho_{,min}$ = 0.2%.

The wall capacity evaluated according to EC8 provisions for medium ductility class structures (DCM), by adopting mean mechanical properties values, should lead to a bending failure in correspondence of a shear force equal to 708 kN (being the web shear and sliding strength equal to 1742 kN and 924 kN, respectively). The same evaluation carried out according to EC8 provisions for high ductility class structures (DCH) leads to a diagonal tension failure of the web reinforcement in correspondence of a shear force equal to 631 kN (being the sliding strength equal to 1930 kN). Experimentally the collapse mechanism, that occurred at a total applied force equal to 764 kN, was governed by shear with the formation of a large crack near the base section, leading to a failure of the longitudinal web reinforcement.

The specimen was modelled with the fixed crack model PARC_CL and shell elements. The NLFE analysis demonstrated that the collapse occurred for a shear failure of the web reinforcement with the formation of a large crack nearby the base section, due to low reinforcement ratio of the web. Fig.10 shows that the model is in good accordance with the experimental test both in terms of crack patterns and failure load. This example demonstrates that shell model is particularly adequate for the evaluation and influence of the detailing of the wall when analytical calculation could lead to a misinterpretation of the real failure mechanism.

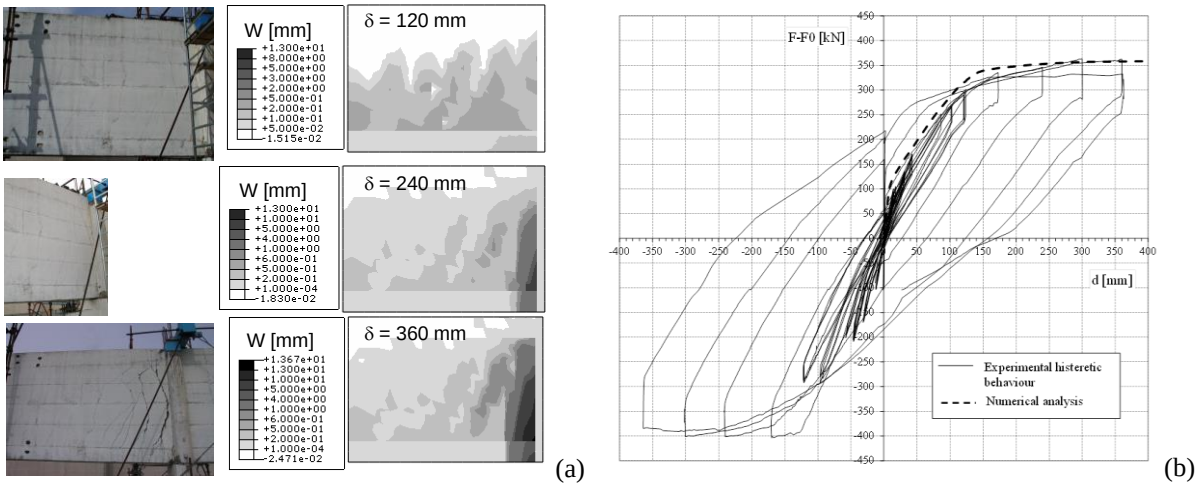

Figure 10. (a) Comparison between experimental and numerical crack pattern of the tested wall; (b) net force F-F0 at one actuator (where F0 is the force needed to equilibrate the selfweight) vs top displacement curve.

3.3 Squat walls

For shear-critical specimens, aggregate interlock, tension stiffening, multiaxial stress states and Poisson effects play all an important role in the structural response. This is particularly true for squat walls, often used in low rise structures. It is common that aspect ratio are equal to 0.5 or even lower. Due to their brittelness, many uncertainties are related to the seismic behaviour and failure mechanisms predictions of this type of structural system. Furthermore for these structures the performance requirements and compliance criteria for damage limit state (DLS) verification can be more severe than the ones for ultimate limit state (ULS). For this reason it is fundamental the use of a model that can properly evaluate the actual crack pattern, like a shell element modelling. In this paper a case study of a squat wall which refers to the Concrack International Benchmark (2011), Fig. 11, has been analysed with strut and tie model, variable inclination truss model and NLFE analyses carried out by applying the constitutive model PARC_CL implemented in ABAQUS Code and with the software DIANA.

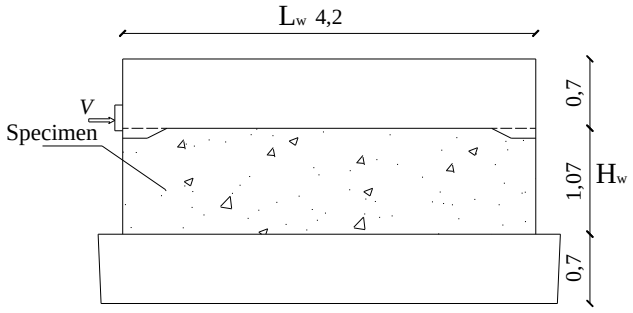

Figure 11. Specimen geometry.

Table 2. Materials and geometrical parameters.

Parameter	Value
f_{cm}	42.5 MPa
f_{ck}	34.5 MPa
h_w	1.07 m
l_w	4.20 m
t_w	0.15 m

For the analyses performed with DIANA both a total strain fixed and rotating crack models have been adopted. A variable Poisson's coefficient that linearly decreases from 0.19, in the elastic phase, up to 0.0 as the residual tensile stress is 0.0, has been used. The biaxial state of stresses has been considered by adopting a maximum reduction of the compressive strength due to lateral cracking of 40% ($f_{c,red}/f_c$=0.6). The tensile fracture energy G_f has been evaluated according to Model Code 2010, while in case of fixed crack model, a variable shear retention factor decreasesing from 1, in the elastic phase, up to 0.0 has been adopted.

In order to underline the effects of phenomena that occur after cracking, a preliminary set of analyses have been carried out with PARC_CL model. First, only the mechanical contributions given by concrete and steel was taken into account (Analysis A), secondly the contribution of aggregate interlock (Analysis B) has been added and finally tension stiffening (Analysis C) has been considered. The three analyses are compared in terms of load versus displacement curve in Fig.12 (a).

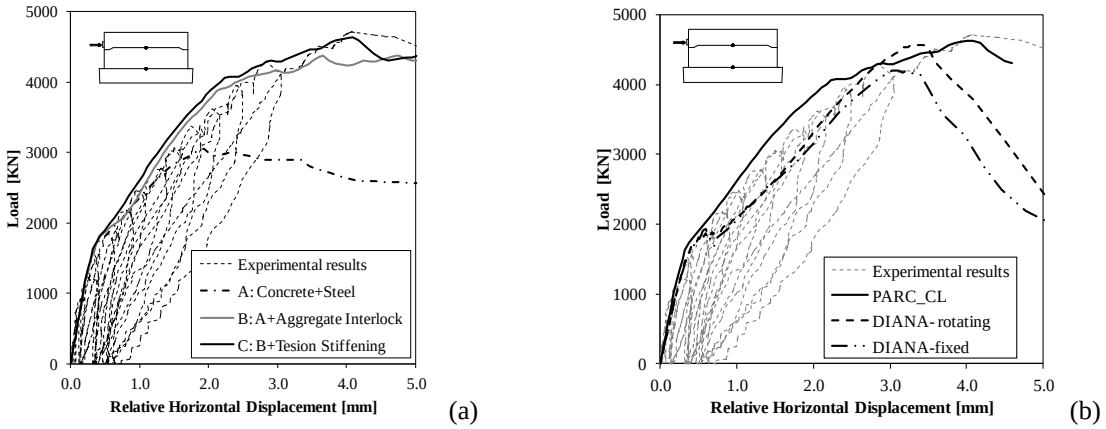

Figure 12. (a) Comparison of the preliminary set of analyses carried out with PARC_CL model, (b) Load-displacement curves: comparison between PARC_CL and DIANA models

By comparing analyses A and B, it is possible to note the large influence of the aggregate interlock, while by comparing analysis B to analysis C, it can be noted that the contribution due to the tension stiffening is not relevant in this case. The dowel action effect has been neglected in the study, in order to be in the same conditions as DIANA model, in which the dowel action effect is not taken into account. Fig. 12 (b) shows that both ABAQUS model and DIANA models adequately describe the wall behaviour in terms of load vs displacement curves. Due to the different basic hypotheses, in Fig. 12 (b) it is possible to observe a little difference in terms of peak load and stiffness of the structure in the cracked phase for the NLFEA curves obtained with fixed crack model and rotating crack model implemented in DIANA code. The ultimate load evaluated with NLFE analysis corresponds to crushing of concrete near the loading steel plate, as experimentally observed, Fig. 13.

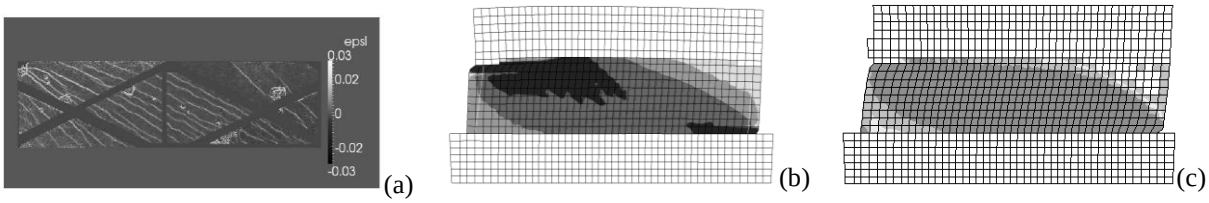

Figure 13. Comparison among (a) experimental, (b) PARC_CL and c) DIANA crack patterns.

The peak load is well predicted both with PARC_CL model and with the rotating crack model of DIANA. The greatest difference between the two models is in the stiffness of the structure in the cracked phase and in the peak deformation. Indeed the different modeling of the biaxial state of stresses and the aggregate interlock effect in PARC_CL model and in DIANA model leads to some differences in the structural prediction.

The results obtained with NLFEA are compared with the results obtained with analytical strut and tie methods. All the analytical calculations refer to mean mechanical properties of materials, Table 2. The tested specimen has an aspect ratio equal to 0.25, then according to EC8 can be defined as a large wall. EC8 provisions simply give a suitable value for the evaluation of the strut width which should not exceed $0.25l_w$ or $4b_w$. In this case the strut width is equal to $a_s=min\{0.25l_w;4b_{w0}\}=4b_{w0}=600$mm where l_w is the wall length and b_{w0} is its width. According to Model Code 2010 formulation the reduced concrete compression strength is equal to:

$$f_{c,strut}=\frac{k_c f_{ck}}{\gamma_c}=20.8MPa \quad with \quad k_c=0.55\eta_{fc}=0.49 \quad \eta_{fc}=\left(\frac{30}{f_{ck}}\right)^{1/3}=0.89\le 1.0 \tag{11}$$

Finally, the shear force correspondent to the compressive failure of the strut is equal to 1676 kN. In Paulay and Priestly (1992) it is suggested another formulation for the evaluation of the strut width, given by Eq.(12):

$$a_s = \left(0.25 + 0.85\frac{N_c}{A_c f_c}\right)\cdot l_w \quad (12)$$

If Eq.(12) is adopted and considering that the axial force N_c on the specimen is approximately equal to 0, the strut width is then equal to $0.25l_w$=1050 mm. The correspondent maximum shear force compression strength is equal to 2931 kN. The shear capacity can also be evaluated in accordance to EC8 with a variable inclination truss model. Squat walls cannot rely on energy dissipation and consequently must be designed as DCM structures. Hence the shear strength can be evaluated according to the formula used for the calculation of shear strength in columns. According to the provisions of EC8 the shear strength is then equal to 4734 kN (for cotθ=1.45). Moreover, since sliding shear strength results equal to 3315 kN, lower than the web shear stress, the failure mode prediction is related to sliding.

4 CONCLUSIONS

In the paper a brief review of the state of the art on squat walls and slender walls design has been presented together with NLFE method approaches. The main remarks are listed in the following:

- Alternative procedures to satisfy performance requirements and compliance criteria for RC walls resisting systems (modelled with shell elements) that circumvent the use of generalized stresses (N, M, V) could be proposed for NLFE software users.
- The proposed verifications can be performed in terms of global and local engineering demand parameters like displacements, material stresses and crack opening values limitations for damage limit state verifications. For ultimate limit state verifications the proposed verifications can be performed in terms of displacements and strain for confined, un-confined concrete and for steel in tension and compression (considering also rebars buckling phenomena and second order effects in general).
- Shell model demonstrates to be a useful numerical tool to properly predict the indicators of damage, fundamental for the application of performance-based earthquake engineering in structural wall systems.

5 REFERENCES

Barda F, Hanson J.M., Corley W.G (1977) “Shear strenght of low rise walls with boundary elements”, Reinforced concrete structures in Seismic Zones, ACI Special Publications 53: 149-202

Belletti, B., R. Cerioni, and I. Iori (2001) “Physical approach for reinforced-concrete (PARC) membrane elements”. *Journal of Structural Engineering*, ASCE, 127(12): 1412-1426

Belletti B., Riva P (2008) “Alcune applicazioni del modello “PARC” all’analisi statica non lineare di edifici a pareti in calcestruzzo armato soggetti ad azioni sismiche”, *Proceedings of the XVII CTE*, 39-48 Rome, 5-8 November, Italy (in Italian)

Belletti, B., and Esposito, R (2010). “Un modello costitutivo per elementi in C.A. soggetti ad azioni cicliche.” Proc., 18th C.T.E. Conf., Brescia, Italy, 81–91 (in Italian)

Belletti B, Esposito R, Damoni C (2013[a]) “Numerical prediction of the response of a squat shear wall subjected to monotonic loading through PARC_CL model”, *Proceeding of the VIII International Conference on Fracture Mechanics of Concrete and Concrete Structures FraMCoS-8*, Toledo, Spain

Belletti B, Esposito R, Walraven J (2013[b]). “Shear Capacity of Normal, Lightweight, and High-Strength Concrete Beams according to ModelCode 2010. II: Experimental Results versus Nonlinear Finite Element Program Results”. *ASCE Journal Of Structural Engineering*, 139(9), 1600-1607

Belletti B, Damoni C, Gasperi A (2013[c]) “Modeling approaches suitable for pushover analyses of RC structural wall buildings”, *Engineering Structures*,57, pp. 327-338

Biaxial software, free download from www.reluis.it

CEB-FIP Bulletin d'Information 65&66 - Model Code MC2010

Damoni C, Belletti B, Lilliu G (2013) “Control of cracking in RC structures: numerical simulation of a squat wall”, *Proceeding of the VIII International Conference on Fracture Mechanics of Concrete and Concrete Structures FraMCoS-8*, Toledo, Spain

Farvashany F.E (2004) Strength deformation of high strength concrete shear walls Ph.D.Thesis, department of civil engineering, Curtin University f Technology, Curtin, Australia

Filippou F.C., Popov E.P. and Bertero V.V., (1983) "Modelling of R/C joints under cyclic excitations," Journal of Structural Engineering, Vol. 109, No. 11, pp. 2666-2684

Gambarova P.G (1983) “Sulla trasmissione del taglio in elementi bidimensionali piani di C.A. fessurati.” *Proc., Giornate AICAP*, pp. 141–156

Greifenhagen C (2006) Seismic behavior of lightly reinforced concrete squat shear walls Ph.D.Thesis, École Polythecnique Federal de Lousanne, Switzerland

Gulec C.K, Whittaker A.S (2009) “Performance-Based Assessment and Design of Squat Reinforced Concrete Shear Walls”, Technical Report MCEER-09-0010, University at Buffalo, State University of New York

Gupta A, Rangan V (1998) “High-strength concrete (HSC) structural walls”, *ACI Structural Journal* 95(2): 194–204

Hendriks M.A.N, Uijl J.A, De Boer A,. Feenstra P.H, Belletti B, Damoni C (2012) “Guidelines for non-linear finite element analyses of concrete structures”, Rijkswaterstaat Technisch Document (RTD), Rijkswaterstaat Centre for Infrastructure, RTD:1016:2012

Hwang S.J, Chiou T.C, Tu Y.S (2004) “Reinforced concrete squat walls retrofitted with carbon fiber reinforced polymer”, *Proceeding of the 2nd International Conference on FRP Composites inCivil Engineering - CICE*, Adelaide, Australia, 621-629

Ile N, Reynouard J.M (2005) “Behaviour of U-Shaped walls subjected to uniaxial and biaxial cyclic lateral loading”, *Journal of earthquake Engineering*, 9(1): 67-94

Kabeyasawa T, Hirahishi H (1998) “Tests and Analyses of high-strength reinforced concrete shear walls in Japan” *ACI Special Publication*, 176-13: 281–310

Kent, D.C. and Park, R. (1971) “Flexural members with confined concrete”. *Journal of Structural Division*, Proceedings of the American Society of Civil Engineers, 97, pp. 1969-1990

Leonhardt F, Schelling G (1974) “Torsionsversuche an Stahlbe-tonbalken”, *vo Deutscher Ausschuss fur Stahlbeton*, 239, Ernest & Sohn, Berlin (in German)

Lefas I.; Kotsovos, M.; Ambraseys, N (1990) “Behavior of Reinforced Concrete Structural Walls: Strength,Deformation Characteristics, and Failure Mechanism” *ACI Structural Journal*, 87(1): 23–31

Maier J, Thurlimann B (1985) “*Bruchversuche an Stahlbetonscheiben*”, IBK Bericht 8003-1, ETH Zurich, Institut fur Baustatik und Konstruktion (in German)

Mander J.B., Priestley M.J.N. and Park R. (1988) "Theoretical stress-strain model for confined concrete,"Journal of Structural Engineering, Vol. 114, No. 8, pp. 1804-1826

Mazars J, Kotronis P, Davenne L (2002) “A new modelling strategy for the behaviour of shear walls under dynamic loading” *Earthquake engineering and structural dynamics*, 31(4) pp. 937-954

Menegotto M. and Pinto P.E., (1973) "Method of analysis for cyclically loaded R.C. plane frames including

changes in geometry and non-elastic behaviour of elements under combined normal force and bending," *Symposium on the Resistance and Ultimate Deformability of Structures Acted on by Well Defined Repeated Loads*, International Association for Bridge and Structural Engineering, Zurich, Switzerland, pp. 15-22

Naze P.A., Sidaner, J.F. (2001). “*Presentation and Interpretation of SAFE Tests: Reinforced Concrete Walls Subjected to Shearing*” SMiRT 16, August, Washington, D.C.

Martinelli P (2007) Shaking Table Tests on RC Shear Walls: significance of numerical Modeling, Ph.D.Thesis, Politecnico di Milano, Italy

Oesterle R. G, Fiorato A. E, Johal L. S, Carpenter J. E, Russell H. G, Corle, W. G (1976) “Earthquake-resistant structural walls—Tests of isolated walls.” Rep. National Science Foundation, Construction Technology Laboratories, Portland Cement Association,Skokie, Ill

Palermo D, Vecchio F.J (2002) Behavior of three-dimensional reinforced concrete shear walls, ACI Structural Journal 99(1) pp. 81–89

Palermo D, Vecchio F.J (2007) “Simulation of Cyclically Loaded Concrete Structures Based on the Finite-Element Method”, *Journal of Structural Engineering*, 133:728-738

Pilakoutas, K.; Elnashai, A. S.: Interpretation of testing results for reinforced concrete panels, ACI Structural Journal 90(6) (1993) pp. 642–645

Paulay T, Priestly M.J (1992) “Seismic design of reinforced concrete and masonry buildings”, *Wiley, New York.*

Riva P, Meda A, Giuriani E (2003) “Cyclic behaviour of a full scale RC structural wall”, *Engineering Structures*, 25: 835-845

UNI EN 1998-1-8:2005. Eurocode 8: design of structures for earthquake resistance

Vecchio F. J., and Collins M. P (1993) “Compression response of cracked reinforced concrete” *Journal of Structural Engineering*, 119(12): 3590–3610

Whyte C.A, Stojadinovic B (2013) “Hybrid Simulation of the Seismic Response of Squat Reinforced Concrete Shear Walls”, PEER Report 2013/02 Pacific Earthquake Engineering Research Center Headquarters at the University of California, Berkeley

Wood S.L (1990) “Shear strength of Low-Rise Reinforced Concrete Walls”, *ACI Structural Journal*, 87(1):99-107